Developmental Cell
Article

SATB1 Defines the Developmental Context for Gene Silencing by *Xist* in Lymphoma and Embryonic Cells

Ruben Agrelo,[1] Abdallah Souabni,[1] Maria Novatchkova,[1] Christian Haslinger,[2] Martin Leeb,[1] Vukoslav Komnenovic,[1] Hiroyuki Kishimoto,[1] Lionel Gresh,[1] Terumi Kohwi-Shigematsu,[3] Lukas Kenner,[4] and Anton Wutz[1,*]
[1]Research Institute of Molecular Pathology, Dr. Bohr-Gasse 7, A-1030 Vienna, Austria
[2]Boehringer Ingelheim Austria, A-1121 Vienna, Austria
[3]Life Sciences Division, Lawrence Berkeley National Laboratory, University of California, Berkeley, Berkeley, CA 94720, USA
[4]Institut für klinische Pathologie, Währinger Gürtel 18-20, and LBI-CR, Währingerstrasse 13A, A-1090 Wien, Austria
*Correspondence: wutz@imp.univie.ac.at
DOI 10.1016/j.devcel.2009.03.006

SUMMARY

The noncoding *Xist* RNA triggers silencing of one of the two female X chromosomes during X inactivation in mammals. Gene silencing by *Xist* is restricted to a special developmental context in early embryos and specific hematopoietic precursors. Here, we show that *Xist* can initiate silencing in a lymphoma model. We identify the special AT-rich binding protein SATB1 as an essential silencing factor. Loss of SATB1 in tumor cells abrogates the silencing function of *Xist*. In lymphocytes *Xist* localizes along SATB1-organized chromatin and SATB1 and *Xist* influence each other's pattern of localization. SATB1 and its homolog SATB2 are expressed during the initiation window for X inactivation in ES cells. Importantly, viral expression of *SATB1* or *SATB2* enables gene silencing by *Xist* in embryonic fibroblasts, which normally do not provide an initiation context. Thus, our data establish SATB1 as a crucial silencing factor contributing to the initiation of X inactivation.

INTRODUCTION

Mammals compensate the different number of X chromosomes between the sexes by X inactivation. One of the two female X chromosomes becomes transcriptionally silent in a developmentally regulated manner. The noncoding *Xist* RNA, which localizes to the inactive X chromosome (Xi), initiates chromosome-wide gene repression. *Xist* is required for the initiation of X inactivation in early embryonic cells (Marahrens et al., 1997; Penny et al., 1996), whereas in most differentiated cells the Xi is silenced in a stable manner which is independent of *Xist* (Brown and Willard, 1994; Csankovszki et al., 1999). Therefore, X inactivation is separated into an initiation and a maintenance phase. Several factors that act in maintaining the silent state of the Xi have been identified, including the histone variant macroH2A (Costanzi and Pehrson, 1998; Mermoud et al., 1999; Rasmussen et al., 2000), histone H4 hypoacetylation (Keohane et al., 1996), and DNA methylation (Sado et al., 2000, 2004). Recently, it has been shown that the SmcHD1 protein is required for maintenance of DNA methylation patterns and gene repression on the Xi (Blewitt et al., 2008).

At the initiation of X inactivation chromosome-wide silencing by *Xist* is initially reversible. In embryonic stem (ES) cells reactivation of genes can be observed when *Xist* expression is abolished (Wutz and Jaenisch, 2000). Gene silencing depends on the 5′-end of *Xist* which contains the repeat A sequence motif (Wutz et al., 2002). Mutation of repeat A abolishes the gene silencing function of *Xist*, but has no effect on *Xist* localization to the chromosome. Several factors that have been observed enriched on the Xi, such as Polycomb group complexes, are recruited by *Xist* in the absence of repeat A. This shows that these factors are not sufficient for gene repression, suggesting that an additional pathway is engaged in the initiation of chromosome-wide silencing (Plath et al., 2003; Schoeftner et al., 2006). No primary initiation factors have been identified to date.

The gene silencing function of *Xist* is restricted to cells of the early embryo (Savarese et al., 2006). In most differentiated cells, where the Xi is stably silenced, *Xist* expression can not initiate gene silencing (Sado et al., 2004; Savarese et al., 2006; Wutz and Jaenisch, 2000). We have previously observed that *Xist* expression can initiate gene silencing in lineage-restricted progenitor cells in the hematopoietic system of adult mice (Savarese et al., 2006). Thus, a special developmental context in the early embryo and the hematopoietic system exists in which chromosome-wide silencing can be established. Why *Xist* expression cannot establish silencing outside these developmental windows is unknown. One possibility is that expression of essential silencing factors is restricted to specific developmental contexts. We reasoned that perhaps we could find initiation factors by setting a condition where *Xist* could silence outside the known developmental windows.

RESULTS

Xist Initiates Ectopic X Inactivation in Lymphoma Cells and Blocks Tumor Growth

To assess whether an epigenetic context for *Xist*-mediated silencing exists in cancer cells we used an inducible *Xist* allele (TX), in which a tetracycline-inducible promoter is inserted

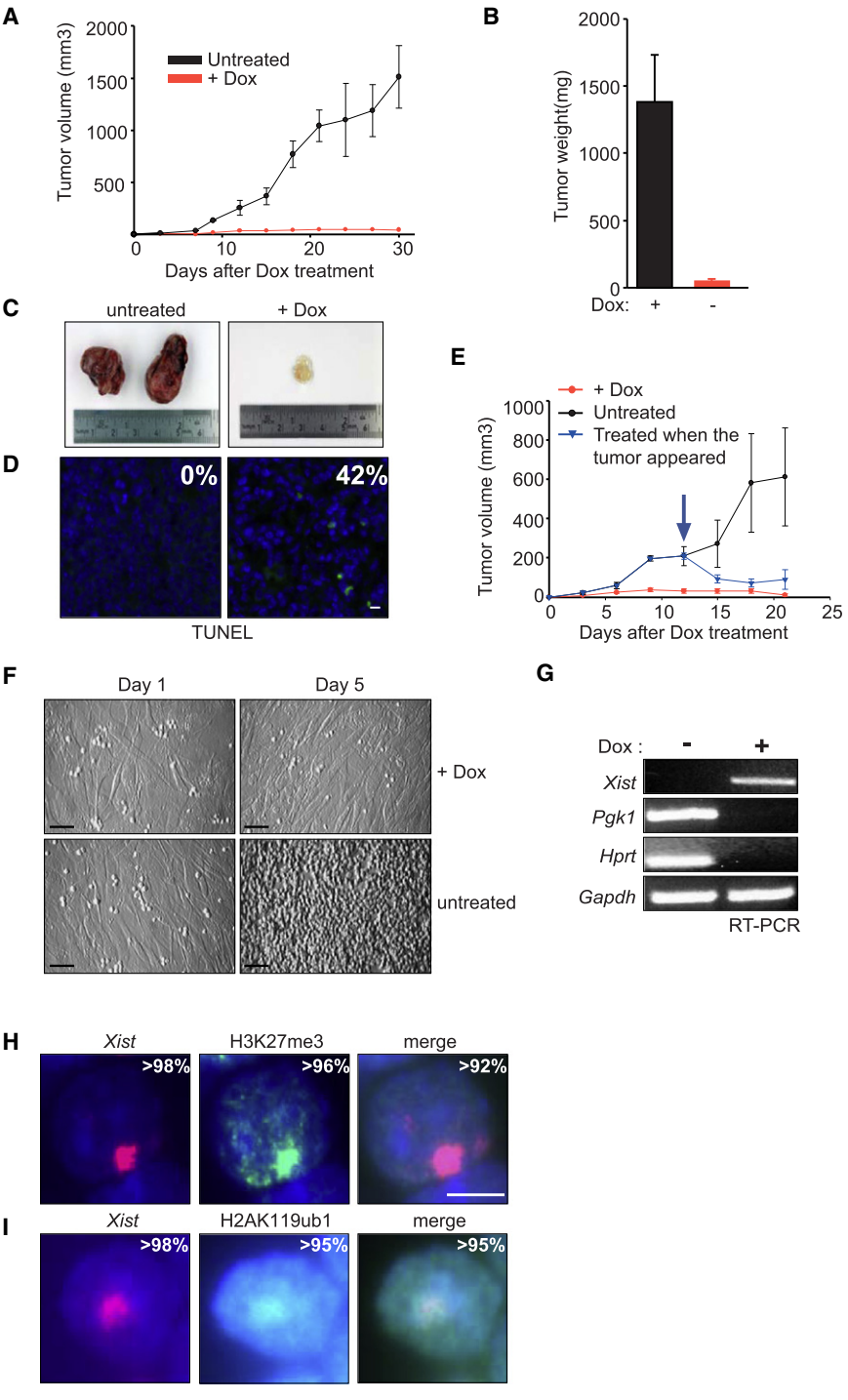

Figure 1. *Xist* Initiates Ectopic X Inactivation in Lymphoma Cells and Blocks Tumorigenesis

(A) Tumor growth was monitored in Doxycycline (Dox)-treated (red) and untreated (black) nude mice after subcutaneous injection of 2 × 10^6 NPM-ALK TX/Y R26$^{rtTA/rtTA}$ lymphoma cells (n = 10). Error bars represent standard deviation.

(B) Tumor weight on Day 30 (n = 10).

(C and D) Tumor morphology (C) and TUNEL analysis ([D], green) of histological tumor sections showing apoptotic cells in the Dox-treated mice. Nuclei are counterstained with DAPI (blue). Scale bar = 10 μm.

(E) *Xist* induction on day 12 after tumor graft (blue arrow) causes remission of established tumors (blue). Untreated tumors (black) and tumors treated with Dox from day 2 after tumor graft (red) are controls (n = 10). Error bars represent standard deviation.

(F) NPM-ALK TX/Y R26$^{rtTA/rtTA}$ lymphoma cell cultures on feeders on days 1 and 5 with and without Dox. Scale bar = 50 μm.

(G) RT-PCR showing silencing of the X-linked *Pgk1* and *Hprt* genes after 48 hr of ectopic *Xist* induction in NPM-ALK TX/Y R26$^{rtTA/rtTA}$ lymphoma cells.

(H and I) Combined RNA FISH immunofluorescence analysis showing colocalization of H3K27me3 (H) and H2AK119ub1 (I) with *Xist* RNA. Percentage of total cells is given in the panels (n = 500). Scale bar = 5 μm.

upstream of the *Xist* transcription start (Savarese et al., 2006). Induction of *Xist* expression from the single X chromosome in TX/Y males causes X inactivation and consequently loss of X-linked genes leads to cell death in the context of T cell progenitors, particularly CD4$^+$ CD8$^+$ thymocytes (Savarese et al., 2006). We introduced the TX allele into a thymic lymphoma model, which is triggered by an oncogenic NPM-ALK fusion protein under the control of a CD4 promoter (Chiarle et al., 2003). The NPM-ALK protein results from the fusion of the anaplastic lymphoma kinase (ALK) to the nucleophosmin (NPM/B23) gene by a t(2;5) translocation found in human anaplastic large cell lymphoma (ALCL; Chiarle et al., 2008; Morris et al., 1994). We generated mice carrying the NPM-ALK transgene, which were either hemizygous TX/Y males or homozygous TX/TX females for the inducible *Xist* allele and homozygous for the Doxycycline-inducible transactivator R26$^{rtTA/rtTA}$ expressed from the ROSA26 locus (Savarese et al., 2006). Thymic lymphomas developed 6–12 weeks after birth and consisted of Thy 1.2$^+$ B220$^-$ cells, which were mostly CD4$^+$ CD8$^+$ and in some cases CD4$^-$ CD8$^-$. To measure the effect of *Xist* induction on tumor growth we injected 1 × 10^6 lymphoma cells subcutaneously into immunedeficient athymic nude mice using Matrigel as a carrier (Azuma et al., 2005). Untreated recipient mice developed lymphomas in all injection sites, whereas *Xist* induction by Doxycycline completely blocked tumor growth (Figures 1A–1C; see Figures S1D and S1E available online). TUNEL staining indicated that *Xist* induction triggered tumor cell death (Figure 1D). Comparable results were obtained with several independent primary lymphoma isolates including a female tumor with a homozygous TX allele, where *Xist* could be induced from both X chromosomes (Figure S2). To examine

if *Xist* induction causes tumor regression, we administered Doxycycline after tumor establishment. When Doxycycline was administered 12 days after the graft, tumor remission was observed (Figure 1E). A control NPM-ALK X/Y R26$^{rtTA/rtTA}$ tumor that does not carry the TX allele was unaffected by Doxycycline treatment showing that tumor ablation was an effect of *Xist* induction (Figure S3).

We confirmed these results with a second tumor paradigm and injected 2 × 10^6 NPM-ALK TX/Y R26$^{rtTA/rtTA}$ lymphoma cells into the tail vein of Rag2$^{-/-}$ common-$\gamma^{-/-}$ immune compromised mice. After 21 days mice treated with Doxycycline were healthy and tumor-free, while untreated recipients showed massive infiltration of tumor cells in several organs (Figure S4).

To investigate if *Xist* induction caused ectopic X inactivation, we established several cell lines by culturing primary tumors in the presence of IL-7 on OP9-derived feeder cells. We plated 3 × 10^5 cells and measured cell growth in the presence or absence of Doxycycline. We observed that *Xist* induction from the single male X chromosome (TX/Y) or both female X chromosomes (TX/TX) caused a loss of tumor cells (Figure 1F and Figure S5A), whereas Doxycycline had no effect on control tumor cells without the TX allele. Doxycycline treated male NPM-ALK TX/Y R26$^{rtTA/rtTA}$ lymphoma cells showed *Xist* expression and a marked loss of the X-linked gene expression (Figure 1G). *Xist* clusters were detected in 98% of the cells induced with Doxycycline, whereas no *Xist* focus was detected without induction (Figure S5B). In over 90% of the cells *Xist* colocalized with trimethylated histone H3 lysine 27 (H3K27me3) and histone H2A ubiquitinated on Lysine 119 (H2AK119ub1), which are two prominent markers of the Xi (Figures 1H and 1I). These data showed that *Xist* induction triggered ectopic X inactivation in lymphoma cells equivalent to embryonic cells.

Identification of *SATB1* as a Silencing Factor for *Xist*

We reasoned that the lymphoma context might provide an opportunity for identifying initiation factors for *Xist*. For this we aimed at generating a tumor that is resistant to *Xist*-mediated killing. Tumor resistance is known to arise for virtually any therapeutic agent. Surprisingly, resistance to *Xist*-mediated killing was not observed in our tumor grafts despite considerable efforts. Therefore, we cultured lymphoma cells for 1 month in the absence of Doxycycline to trigger tumor cell evolution. Then 2 × 10^6 NPM-ALK TX/Y R26$^{rtTA/rtTA}$ cells were transplanted into the flank of nude mice and tumor development was studied in the presence of Doxycycline. Initially treated mice showed no signs of tumor growth in stark contrast to control mice that did not receive Doxycycline (Figure 2A). This is consistent with the large majority of tumor cells being ablated by *Xist* induction. However, after 21 days tumors started to appear at all injection sites in Doxycycline-treated mice (Figure 2A and Figure S6A). It is likely that these tumors originated from rare cells that acquired resistance to *Xist*-mediated killing during in vitro culture. In histological tumor sections *Xist* clusters colocalizing with H3K27me3 foci were observed (Figure 2B). The X-linked *Pgk1* and *Hprt* genes were expressed at a level above or equal to that observed in untreated control tumors or thymic cells (Figure 2C). The presence of one X chromosome per tumor cell was confirmed by X chromosome painting ruling out the possibility that the resistance to *Xist*-mediated killing was due to rearrangement or gain of X chromosomes (Figure S6B). Furthermore, *Xist* induction by addition of Doxycycline did not affect proliferation of a cell line established from this tumor (Figure S6C). These results suggested that spontaneous resistance had arisen by loss of the pathways required for the silencing function of *Xist*.

To identify genes that were associated with resistance to *Xist*-mediated killing we performed genome-wide expression profiling of *Xist*-responsive and *Xist*-resistant tumors and of thymus (Figure 2D and Figure S7). Among the most significantly downregulated genes in resistant tumors (Table S1) we noted *SATB1*, a nuclear protein which functions in regulating chromatin structure and gene regulation in thymocytes (Dickinson et al., 1992; Alvarez et al., 2000; Cai et al., 2003). In thymus, expression of SATB1 is high in the CD4$^+$ CD8$^+$ double-positive T cell compartment, which we previously observed to possess the context for initiation of gene silencing by *Xist* (Savarese et al., 2006). This suggested a correlation of SATB1 expression and gene silencing by *Xist*.

SATB1 Is Essential for the Silencing Function of *Xist* in Thymocytes

To verify that SATB1 could be a limiting factor for the silencing function of *Xist* we analyzed expression in development. In thymus, high levels of SATB1 were found in the cortex, which is predominantly composed of CD4$^+$ CD8$^+$ thymocytes, whereas in the medulla fewer cells showed expression (Figures S8A and S8B). This is consistent with a loss of SATB1 expression upon further thymocyte differentiation to single positive T cells. To test that SATB1 expressing cells in the thymus provided the context for silencing by *Xist*, we induced *Xist* from the single male X chromosome in TX/Y R26$^{rtTA/rtTA}$ mice. We observed a rapid loss of SATB1 expressing cells upon *Xist* induction consistent with cell death caused by ectopic X inactivation (Figure S8C).

In NPM-ALK thymic lymphoma the normal thymic structure was lost and substituted by blasts, which were positive for the NPM-ALK protein and SATB1 (Figures S8A and S8B). Western analysis confirmed a loss of SATB1 protein in *Xist*-resistant tumors (Figure 3A). SATB1 immunohistochemistry in sections revealed a ring-like pattern in the thymus and *Xist*-responsive tumors, whereas *Xist*-resistant tumors showed no or minimal SATB1 expression (Figure 3B). None of the resistant tumors was positive for SATB1. To test if *SATB1* was required for the gene silencing function of *Xist* in lymphoma cells we performed RNAi. RNAi in lymphoma cells was technically difficult and required the optimization of the protocol. For efficient reduction of SATB1 protein levels we used a double transfection protocol. We transfected NPM-ALK TX/Y R26$^{rtTA/rtTA}$ lymphoma cells with siRNA specific for *SATB1* or control siRNA. After two days *Xist* expression was induced and a second siRNA transfection was performed 3 days thereafter. We measured the total cell numbers of triplicate cultures with and without Doxycycline induction after 5 days and calculated the percentage of surviving cells after *Xist* induction. Cells transfected with *SATB1* siRNAs showed a significantly higher survival compared to controls (Figure 3C and Figure S8D). Western and immunofluorescence analysis showed reduced SATB1 expression in most cells treated with *SATB1* siRNA, but not control siRNA, confirming the effect of the siRNA (Figure 3D and Figure S8E). SATB1 seemed to stabilize *Xist* RNA and thus after RNAi a reduction

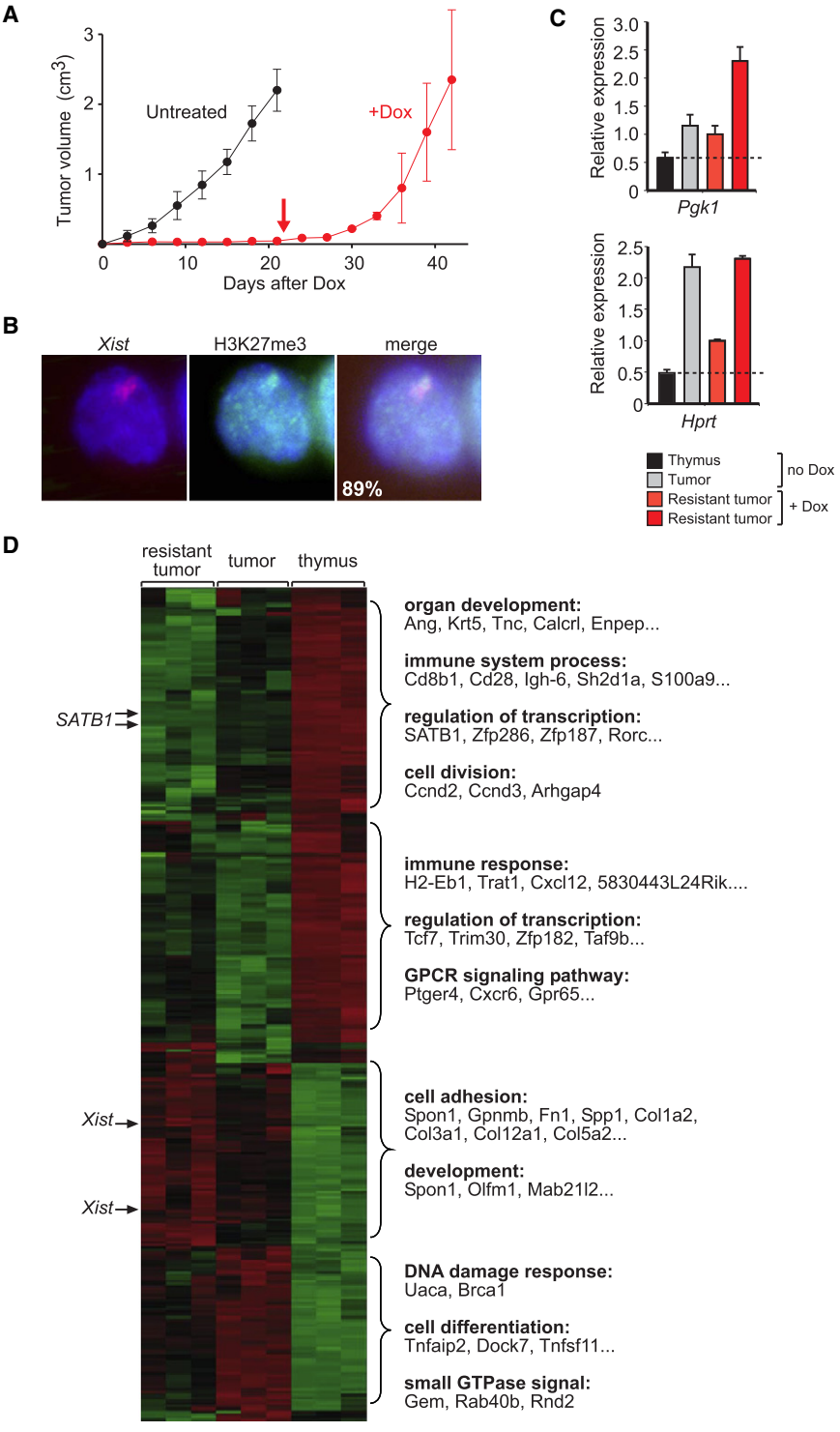

Figure 2. Derivation of an *Xist*-Resistant Tumor for Identification of Silencing Factors

(A) Tumor growth after transplantation of 2 × 10^6 cultured NPM-ALK TX/Y R26$^{rtTA/rtTA}$ lymphoma cells into nude mice. After 22 days (red arrow), *Xist*-resistant tumors appear in the Dox-treated group (red; n = 5). Error bars represent standard deviation.

(B) *Xist* RNA FISH (red) and H3K27me3 (green) in histological sections of the resistant tumor. Percentage of colocalization is given.

(C) Quantitative RT- PCR analysis showing that the X-linked *Pgk1* and *Hprt* genes are still expressed in the resistant tumors when *Xist* is induced with Dox at a comparable level to normal thymus or parental tumor without *Xist* induction. Results were normalized to *Gapdh*. Error bars represent standard deviation (n = 3).

(D) Heatmap showing upregulated (red) and downregulated (green) genes after hierarchical clustering of gene expression profiles of *Xist*-resistant and *Xist*-responsive NPM-ALK TX/Y R26$^{rtTA/rtTA}$ lymphoma and normal male thymus. Probes for *Xist* and *SATB1* are indicated (arrows) and gene groups are annotated (right).

in *Xist* signal was observed (Figure S8E). We believe that *Xist* can localize onto SATB1 organized chromatin and is thereby stabilized leading to higher *Xist* levels. However, we also note that in the *SATB1* siRNA-treated cells we observed efficient *Xist* induction.

To test if SATB1 is sufficient to restore *Xist* silencing in the resistant tumor we virally expressed *SATB1* in a cultured *Xist*-resistant tumor cell line. SATB1 expressing tumor cells showed a strongly reduced survival upon *Xist* induction compared to *Xist*-resistant tumor cells infected with empty vector (Figures 3E and 3F). Taken together these data strongly support a crucial function for SATB1 in gene silencing by *Xist* in the lymphoid and tumor context.

Xist Localizes along Nuclear *SATB1* Structures in Lymphoid Cells

To investigate a potential interaction we performed SATB1 immunofluorescence analysis combined with *Xist* RNA FISH. In thymocyte nuclei SATB1 is observed in a ring-like structure (Cai et al., 2003). We have previously observed that in CD4$^+$ CD8$^+$ T cells, which constitute the hematopoietic context for gene silencing in the thymus, *Xist* does not form a characteristic focus but appears in a diffuse pattern (Savarese et al., 2006). Therefore, we examined thymi from TX/Y R26$^{rtTA/rtTA}$ mice after induction of *Xist* for 24 and 48 hr. *Xist* formed a characteristic focus after 24 hr of induction. However, after 48 hr *Xist* spread along SATB1 in the majority of cells, whereby it did not colocalize with but rather outlined the SATB1 ring (Figure 3G and Figures S9A–S9E). In normal female thymocytes, we observed the expected *SATB1* ring structure and in more than half of the cells *Xist* did not form a focus but localized along the SATB1 ring (Figure S9F). This localization pattern of *Xist* is therefore observed in a physiologically normal cell type.

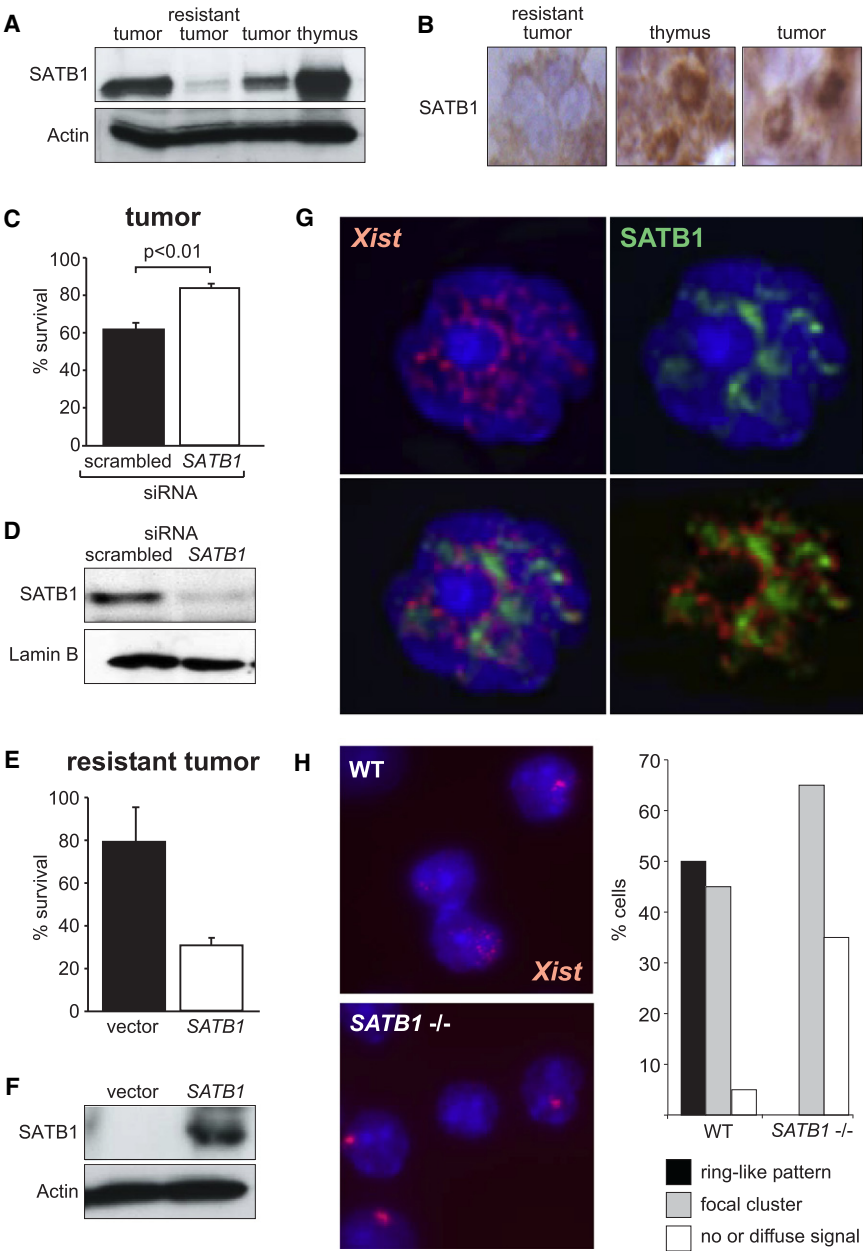

Figure 3. SATB1 Is a Critical Silencing Factor for *Xist* in Lymphoma Cells

(A) Western analysis of SATB1 expression in *Xist*-resistant and *Xist*-responsive tumor and normal thymus. Actin serves as loading control.

(B) Immunohistochemistry in sections reveals nuclear ring-like SATB1 structures in normal thymus and *Xist*-responsive tumor, whereas nuclear SATB1 staining is lost in resistant tumors.

(C) *SATB1* RNAi in cultured NPM-ALK TX/Y R26$^{rtTA/rtTA}$ lymphoma cells significantly increases cell survival after *Xist* induction. Cell survival after 5 days of culture in presence of Dox relative to uninduced cultures is plotted. Scrambled siRNA treatment serves as control (n = 3). Error bars represent standard deviation.

(D) Western analysis confirming loss of SATB1 protein in *SATB1* siRNA treated but not scrambled control siRNA treated cells. Lamin B serves as loading control.

(E) Virally expressed *SATB1* restores *Xist* silencing function in *Xist*-resistant tumor cells. Cell survival after 5 days of cultures in presence of Dox relative to uninduced cultures is plotted. Empty vector-infected cells serve as control (n = 3).

(F) Western analysis confirming SATB1 protein expression in cells infected with *SATB1* but not control virus. Actin serves as loading control.

(G) *Xist* RNA FISH (red) combined with SATB1 immunofluorescence (green) analysis showing *Xist* spreading along the *SATB1* ring in TX/Y R26$^{rtTA/rtTA}$ thymic cells after 48 hr of *Xist* induction with Dox.

(H) Delocalization of *Xist* into a ring-like pattern is observed in thymocytes of wild-type (WT) but not SATB1 deficient female mice. Representative *Xist* RNA FISH images are shown. A statistical analysis of *Xist* patterns in SATB1 deficient and control thymocytes is given (n = 150).

Furthermore, delocalization of *Xist* into a ring-like pattern was not observed in thymocytes isolated from *SATB1*-deficient mice, where more *Xist* foci were observed (Figure 3H). Thus, delocalization of *Xist* in thymocytes depends on SATB1.

Next we induced *Xist* expression in TX/TX R26$^{rtTA/rtTA}$ thymocytes from both female X chromosomes. We observed two *Xist* foci overlapped with two regions of intense SATB1 staining (Figure S9G). Such a focal SATB1 pattern was not observed before induction of *Xist*. This indicated that *Xist* expression from two X chromosomes had caused a redistribution of SATB1 from the ring. Thus, *Xist* and SATB1 apparently interacted and changed each other's localization.

In NPM-ALK TY/Y R26$^{rtTA/rtTA}$ lymphoma cells a characteristic *Xist* focus was observed after 24 hr of induction whereas after 48 hr *Xist* spread along the SATB1 ring (Figures S9H and S10A). We further noted that the Polycomb group proteins Ring1B and Bmi1 were diffusely distributed in the nucleus and showed partial overlap with SATB1 in a ring-like pattern (Figure S10B). We suggest that the interaction between *Xist* and SATB1 in lymphoma cells and in normal thymocytes is potentially mediated by SATB1 organized chromatin. A direct physical attachment is unlikely, as SATB1 and *Xist* RNA showed little overlapping localization.

SATB1 Regulates *Xist* Silencing Function in Embryonic Cells

To analyze if SATB1 is relevant for the initiation of normal X inactivation we analyzed mouse embryonic stem (ES) cells. Western analysis showed SATB1 expression in ES cells, but 3 days after retinoic acid induced differentiation *SATB1* expression became undetectable (Figure 4B). This expression precisely overlaps the window in which *Xist* is able to silence (Wutz and Jaenisch, 2000). Immunofluorescence analysis showed that SATB1 was diffusely distributed and surrounded a characteristic *Xist* focus when *Xist* expression was induced in TX/Y ES cells (Figure 4A)

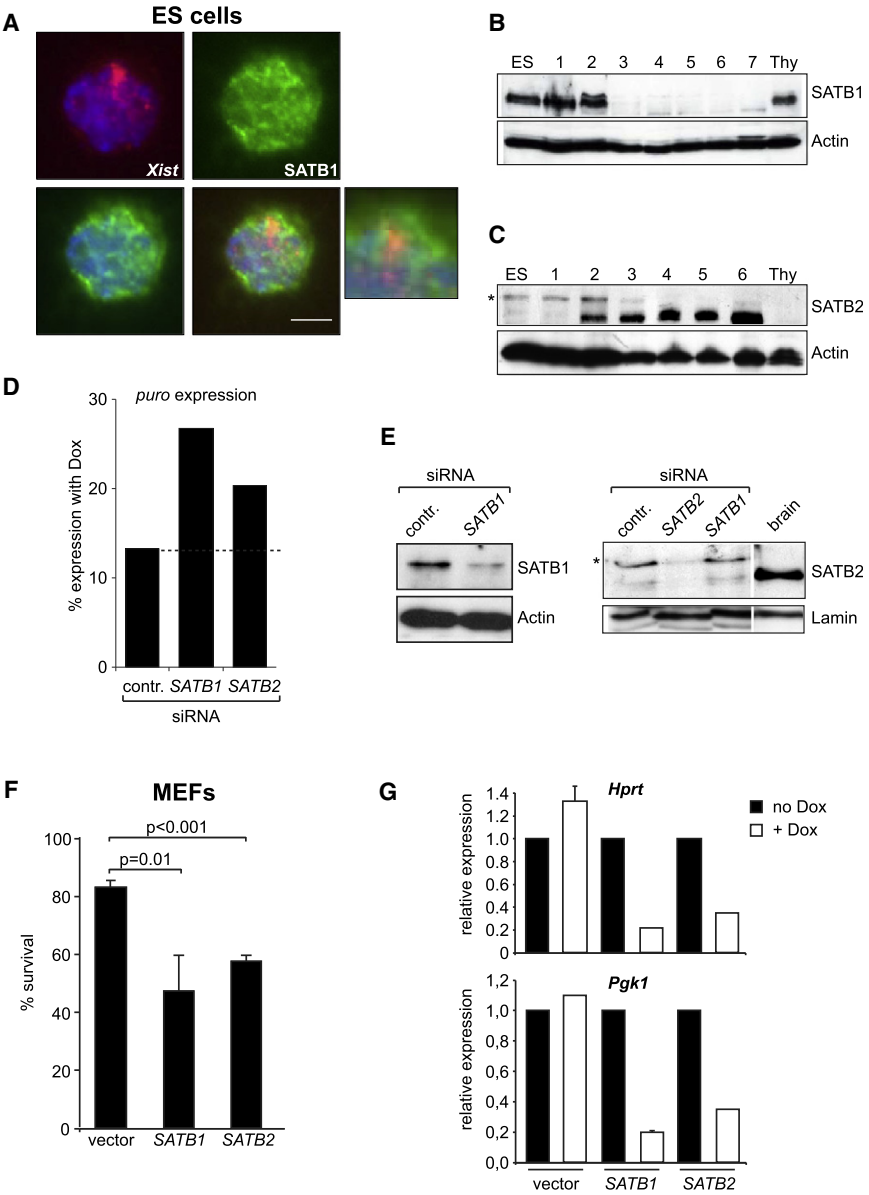

Figure 4. *SATB1* Expression Defines the Silencing Function of *Xist* in Embryonic Cells

(A) Combined RNA FISH immunofluorescence analysis of TX/Y R26$^{rtTA/rtTA}$ ES cells shows SATB1 (green) surrounding the characteristic *Xist* focus (red) after 24 hr of induction with Doxycycline. Scale bar = 5 μm.

(B and C) Western analysis of SATB1 (B) and SATB2 (C) protein during ES cell differentiation shows that SATB1 is lost and SATB2 shifts to a lower molecular weight on day 3, precisely when *Xist* loses its silencing capability. Asterisk indicates the high molecular weight form of SATB2. Actin serves as loading control.

(D) Repression of the puromycin (*puro*) marker, which is cointegrated with an *Xist* transgene on chromosome 11 in clone 36 ES cells, upon *Xist* induction is reduced by *SATB1* or *SATB2* RNAi compared to scrambled control. Quantification of *puro* expression after *Xist* induction relative to uninduced cells is given.

(E) Western analysis demonstrates strongly reduced SATB1 protein in ES cells treated with SATB1 siRNA but not control siRNA. Western analysis of SATB2 in ES cells treated with scrambles control, *SATB2*, and *SATB1* siRNAs. The higher molecular weight form of SATB2 (asterisk) observed in ES cells is depleted by SATB2 RNAi. The lower molecular weight form of SATB2 is observed in brain. Lamin serves as loading control.

(F) Survival of immortalized fibroblasts established from TX/Y R26$^{rtTA/rtTA}$ embryos and infected with *SATB1* and *SATB2* expression vector or control empty vector (vector). The percent survival is calculated from the cell number with *Xist* induction relative to untreated cells (n = 6). Error bars represent standard deviation.

(G) Quantitative RT-PCR showing repression of the X-linked *Hprt* and *Pgk1* genes upon *Xist* induction in MEFs infected with *SATB1* and *SATB2* but not empty vector controls. Expression relative to *Gapdh* is plotted (n = 6). Error bars represent standard deviation.

similar to the endogenous Xi in differentiating female ES cells (Figure S11A). Thus, SATB1 was expressed in the embryonic context for X inactivation and could contribute to the initiation of chromosome-wide silencing. However, disruption of *SATB1* in mice is compatible with female development, suggesting that other factors can take over its function in X inactivation (Alvarez et al., 2000). To test if the close homolog SATB2 could provide such a redundant function, we analyzed its expression in ES cells. Similar to SATB1 we observed SATB2 expression in ES cells (Figure 4C). After 3 days of differentiation, SATB2 showed a switch to a lower molecular weight. The higher molecular weight likely corresponds to a SUMO-modified form that has been previously described as important for gene regulation (Dobreva et al., 2003). The shift in molecular weight at the end of the initiation window of X inactivation suggested that the higher molecular weight form of SATB2 could be important for *Xist* mediated silencing.

To further explore if *SATB1* and *SATB2* contribute to chromosome-wide silencing by *Xist* in ES cells we used RNAi . In clone 36 ES cells an inducible *Xist* transgene leads to repression of a puromycine selection marker, which provides a convenient readout for silencing (Wutz and Jaenisch, 2000). We transfected either control, *SATB1*, *SATB2*, or a combination of *SATB1* and *SATB2* siRNA into ES cells (Figure S11B). While there was little effect of control, *SATB1*, or *SATB2* siRNAs on cell numbers, double RNAi of *SATB1* and *SATB2* led to a cell loss precluding further analysis (Figures S11C and S11D). Analysis of puro expression showed that silencing was efficient in control cells with 13% of puro signal remaining after *Xist* induction. The efficiency of silencing was reduced in cultures treated either with *SATB1* or *SATB2* siRNAs, with 26% and 20% of puro message remaining after *Xist* induction, respectively (Figure 4D). This indicated that an acute loss of SATB1 and SATB2 reduced the efficiency of gene silencing by *Xist* in ES cells. Furthermore,

SATB2 RNAi depleted the high molecular weight form of SATB2 in ES cells confirming that the antiserum was specific (Figure 4E). SATB2 expressed in the brain corresponds to the lower molecular weight form, which we observed in differentiated ES cells after the initiation window. We next asked if SATB1 or SATB2 are limiting for *Xist* silencing function in embryonic cells. We previously reported that induction of *Xist* in embryonic fibroblasts (MEFs) does not cause gene silencing despite normal *Xist* RNA localization (Wutz and Jaenisch, 2000). Thus, MEFs lack essential initiation factors for *Xist*. To establish if either SATB1 or SATB2 would perform as primary initiation factors in the embryonic context, we virally expressed *SATB1* in TX/Y MEFs and tested if gene silencing could be restored. In *SATB1*- and *SATB2*-infected MEFs cell numbers were significantly reduced upon induction of *Xist* expression from the single male X chromosome, whereas *Xist* had no effect on cells infected with a control virus (Figure 4F and Figure S12). Repression of the X-linked *Pgk1* and *Hprt* genes showed that *Xist* induction had indeed led to ectopic X inactivation in *SATB1*- and *SATB2*-infected MEFs (Figure 4G). We conclude that expression of SATB1 or SATB2 substituted an essential primary initiation factor and allowed to reestablish the embryonic context for gene silencing by *Xist* in MEFs.

DISCUSSION

Here we identify SATB1 as a silencing factor for *Xist*. SATB1 is required and sufficient for gene silencing by *Xist* in thymic lymphoma cells. We find that SATB1 is expressed during the initiation window of X inactivation in ES cells and its expression is lost at the time point in differentiation when *Xist* can no longer initiate chromosome-wide silencing. Importantly, viral *SATB1* expression enables gene silencing by *Xist* in mouse embryonic fibroblasts. Expression of SATB1 has also been observed in fetal brain (Alvarez et al., 2000) and in erythroid differentiation (Wen et al., 2005), which is consistent with our previous finding that *Xist* induction leads to ablation of erythroid cells in mice (Savarese et al., 2006). Mutation of *SATB1* in mice leads to misregulation of multiple genes during T cell development and arrests development at the $CD4^+$ $CD8^+$ T cell stage (Alvarez et al., 2000). The development of female mice in the absence of SATB1 demonstrates that other factors can substitute SATB1 function in X inactivation. Thus, SATB1 contributes to X inactivation in embryonic cells together with other potentially as of yet unidentified factors.

We find that one such factor could be SATB2. We observe expression of SATB1 and SATB2 in ES cells. In western analysis SATB1 migrates at its expected molecular weight, whereas there is only a higher molecular weight band for SATB2. This higher molecular weight band is specifically eliminated by *SATB2* RNAi. These data are also consistent with immunofluorescence staining showing SATB2 expression in ES cells, but not thymocytes, which are positive for SATB1 (data not shown). From this we conclude that there is a higher molecular weight form of SATB2 in ES cells. From bioinformatics and *SATB2* transcript analysis we have not found evidence for additional *SATB2* exons. From this we suggest that the higher molecular weight results from posttranslational modification. This is consistent with the shift on Day 2 of ES cell differentiation to the lower molecular weight form corresponding to the unmodified protein. Albeit, western analysis suggests that the lower molecular weight form in differentiated ES cells is more abundant than the higher molecular weight SATB2 in ES cells, we note that this might still be of functional significance since in ES cells SATB1 is also present. Disruption of *SATB2* is also compatible with female development and causes skeletal abnormalities and perinatal lethality in mice (Dobreva et al., 2006; Britanova et al., 2006). SATB2 protein is expressed in the kidney (Dobreva et al., 2003) and the nervous system (Britanova et al., 2005; Dobreva et al., 2003), where we observe the lower molecular form of SATB2 which is not relevant to *Xist* silencing and which might have other functions. SATB2 expression is also reported in pre-B cells (Dobreva et al., 2003), which are efficiently ablated by *Xist* induction in mice (Savarese et al., 2006). The tissue distribution of SATB1 and SATB2 expression is, thus, consistent with a role in enabling chromosome silencing by *Xist*. So far, we have not identified additional proteins with a high sequence homology to *SATB1* and *SATB2* in the mouse genome. Albeit, more work is needed to fully address if other factors than SATB1 and SATB2 contribute to the initiation of X inactivation in the embryo, our data demonstrate a crucial contribution of SATB1 and SATB2 to chromosome-wide silencing by *Xist* and implicate a class of proteins with functions in chromatin organization in the mammalian dosage compensation mechanism.

Our finding that *Xist* spreads along the SATB1 ring in $CD4^+$ $CD8^+$ T cells suggests an interaction that links the localization of SATB1 and *Xist* RNA. This observation could be made in T cells where SATB1 shows a prominent ring- or cage-like staining pattern. In other cell types examined here, SATB1 shows a more diffuse distribution, which makes localization analysis less informative. We further made the intriguing observation that induction of *Xist* from both X chromosomes in TX/TX female thymocytes triggers a change in the localization pattern of SATB1. In these cells SATB1 is localized from a cage-like pattern toward the two *Xist* clusters. This mutual influence on localization suggests that the relative robustness of either the SATB1 cage structure or the chromosome territory organized by *Xist* determine the recruitment of SATB1 to the X chromosome or *Xist* onto SATB1 cage structure.

At the initiation of X inactivation in ES cells we observe SATB1 surrounding the *Xist* domain. Albeit, the precise mechanism of SATB1 in chromosome-wide silencing is not known at present, we suggest a regulatory role of SATB1 for genic chromatin of the X chromosome. *SATB1* has been shown to organize transcriptionally active chromatin into chromatin loops (Galande et al., 2007; Cai et al., 2006). The X chromosome is organized into a gene-rich outer rim and an internal core containing silenced nongenic sequences (Clemson et al., 2006). Chaumeil et al. (2006) showed that genes are moved into the chromosome territory upon silencing in a manner that is dependent on repeat A of *Xist*. It is possible that *Xist* pulls genes into the repressive core compartment for silencing and *SATB1* might act as an anchor in this chromosomal reorganization.

Although we cannot completely rule out that SATB1 acts indirectly in X inactivation via regulation of a target gene, we believe that this is unlikely based on the following evidence: (1) Gain- and loss-of-function experiments of *SATB1* give the expected effect on *Xist* mediated silencing in tumor cells. (2) Expression profiles

of *Xist*-resistant versus *Xist*-responsive tumors did not identify other candidate genes with a chromatin regulatory function or a plausible developmental expression pattern. (3) SATB1 expression in four different cell types enables gene silencing by *Xist*. Since SATB2 also contributes to gene silencing by *Xist*, we deem it extremely unlikely that a common SATB1 and SATB2 target gene is regulating silencing in all cell systems. (4) Our observation of mutual interaction between *Xist* and SATB1 localization in T cells supports a role of SATB1 in chromatin organization for the initiation of chromosome-wide silencing by *Xist*.

We have previously shown that the inactive X chromosome is maintained during the stages in T cell and B cell development when *Xist* can initiate silencing (Savarese et al., 2006). Since *Xist* is delocalized in pre-T cells and very low expression is observed in pre-B cells it is unlikely to contribute to maintaining X inactivation. Since SATB1 can only cause chromosome-wide silencing in combination with *Xist*, this fact strongly indicates that SATB1 is not essential for Xi maintenance in pre-T cells. Furthermore, the fact that the Xi is stably maintained in somatic cells which do not express SATB1 further argues against a general function of SATB1 in the maintenance of X inactivation. Thus, SATB1 is an initiation factor but not a maintenance factor for X inactivation.

SATB1 expression in thymic lymphoma suggests that the epigenetic context of progenitor cells enabling *Xist* gene silencing function is preserved in tumorigenesis. Progenitor-derived leukemia stem cells have also been observed to maintain progenitor identity and reactivate a self-renewal-associated program (Krivtsov et al., 2006). We find SATB1 expressed in a range of human lymphoma types including NPM-ALK positive and negative ALCL (Table S2 and Figure S13). Expression of SATB1 is further associated with more aggressive and poorly differentiated forms of breast cancer in humans (Han et al., 2008). These findings show that the *Xist* gene silencing pathway is also tied in with tumorigenesis. This idea is further consistent with the observation that *XIST* can initiate silencing in a human fibrosarcoma cell line, at least to some extent (Chow et al., 2007; Hall et al., 2002). Understanding the pathway enabling chromosomal silencing by *Xist* in progenitors, thus, might open new perspectives for cancer therapy.

EXPERIMENTAL PROCEDURES

Generation of NPM-ALK Tumors Carrying an Inducible *Xist* Allele, TX

NPM-ALK X/Y transgenic mice (Chiarle et al., 2003) were crossed with TX/TX $R26^{rtTA/rtTA}$ mice (Savarese et al., 2006) to obtain the desired genotypes NPM-ALK TX/Y $R26^{rtTA/rtTA}$ and NPM-ALK TX/TX $R26^{rtTA/rtTA}$. Tumor cells isolated from thymic lymphoma were injected subcutaneously into both flanks of 6-week-old athymic Balb/c nu/nu mice. For each injection, 2×10^7 cells were suspended in 250 μl cold PBS and 250 μl of cold BD Matrigel Basement Membrane Matrix High Concentration (HC). For each experiment, 10 nude mice were injected. *Xist* expression in tumor grafts was induced by administration of Doxycycline via the drinking water (1 g/l Doxycycline and 100 g/l sucrose). Water bottles were protected from light and changed every second day. Tumor development at the site of injection was measured daily. Error bars throughout represent standard deviation unless stated otherwise. Tail vein injection model: single-cell suspensions were prepared from the thymic lymphoma NPM-ALK TX/Y $R26^{rtTA/rtTA}$ mice, and 1×10^6 lymphoma cells were injected into the tail vein of 10 $Rag2^{-/-}$ common-gamma chain $c\gamma^{-/-}$ mice. Five mice were administered Doxycycline and five were not treated. Pathology was analyzed after 21 days.

Cell Culture and Establishment of Lymphoma Cell Lines

ES cells and mouse embryonic fibroblasts were cultured as described previously (Wutz and Jaenisch, 2000). *Xist* expression was induced with 1 μg/ml of Doxycycline. Lymphoma tumor cell lines were established from primary NPM-ALK TX/TX $R26^{rtTA/rtTA}$, NPM-ALK TX/Y $R26^{rtTA/rtTA}$, and NPM-ALK X/Y $R26^{rtTA/rtTA}$ lymphoma. Cells were cultured on murine bone marrow stromal-derived OP9 feeders in IL-7 containing IMDM medium, as described (Hoflinger et al., 2004).

Histology, Immunohistochemistry, and TUNEL Assay

Tumors and normal organs were fixed in 4% neutral buffered formaldehyde at 4°C and embedded in paraffin. Hematoxilin and eosin (H&E) staining was performed on 3 μm sections. Immunohistochemistry was performed with antibodies for ALK (mouse anti-ALK Mab; Zymed), anti-Ki-67 (NCL-Ki67p; Novacostra), or SATB1 (ab49061 Rabbit polyclonal anti-SATB1; Abcam). TUNEL staining was performed by using the in situ cell death detection kit (Roche). Clinical specimens were handled according to institutional guidelines.

RNA Extraction, Reverse Transcription PCR Analysis, and Quantitative PCR Analysis

RNA was isolated using Trizol (Invitrogen, Life Technologies) and further purified using RNeasyTM columns (QIAGEN). Reverse transcription was primed with Oligo(dT)12–18 using the SuperScript II RNase H- RT Kit (Invitrogen). Quantitative PCR was performed for 40 cycles with SYBR Green on an Opticon 2 monitor fluorescence thermocycler (MJ Research, Waltham, MA). Relative concentrations were determined on basis of standard curves of cDNA and normalized for *Gapdh*. Melting curves were run to ensure amplification of a single product. Error bars represent standard deviation. Primers for *Pgk1*, *Hprt*, and *Xist* were previously published (Huynh and Lee, 2003). Primers for *SATB1* were CCTGGATGAGCCCTTTGG and CTGCGTGGTGGAACATTATG and primers for mouse *SATB2* were ACACCGACAACAGACCTC and GGGCTTGAGACACCTTGG. Human *SATB2* primers were as described (Han et al., 2008).

Protein Extraction and Western Blotting

Whole cell extracts prepared with RIPA buffer and western analysis were performed as previously published (Schoeftner et al., 2006) using rabbit anti-SATB1 1:2000 (Dickinson et al., 1992) and SATB2 1:300 (ab34735 rabbit anti-SATB2; Abcam).

Immunofluorescence, RNA FISH, and X Chromosome Painting

ES cells were attached to poly-l-lysine coated coverslips or cytospun using a Cytospin 3 centrifuge (Thermo Shandon, USA). Differentiated cells were grown on Roboz slides (CellPoint Scientific, USA). Lymphoma cells were attached to adhesion slides (Marilienfeld, Germany). Immunostaining was performed as described previously (Leeb and Wutz, 2007). In brief, cells were fixed for 10 min in 4% PFA in PBS, permeabilized for 5 min in 0.1% Na-citrate/0.5% Triton X-100, and blocked for 30 min in PBS containing 5% BSA and 0.1% Tween 20. For H2AK119ub1 immunostaining, cells were pre-extracted in 100 mM NaCl, 300 mM sucrose, 3 mM MgCl2, 10 mM Pipes (pH 6.8), and 0.5% Triton X-100 for 2 min before fixation, and washes after incubation with primary and secondary antibody were performed in KCM buffer (120 mM KCl, 20 mM NaCl, 10 mM Tris [pH 8.0], and 0.5 mM EDTA)/0.1% Tween 20. Antibodies and dilutions for Ring1B, Bmi1, H3K27me3, and secondary antibodies were used as previously published (Leeb and Wutz, 2007). SATB1 antibody (Dickinson et al., 1992) was used in 1:500 dilution. RNA FISH probes were generated by random priming (Stratagene) using Cy3-dCTP (GE Healthcare). After immunostaining, cells were fixed in 4% PFA in PBS for 10 min, dehydrated, hybridized, and washed as described previously (Leeb and Wutz, 2007). Vectashield (Vector Laboratories) was used as imaging medium. X chromosome painting was performed in tissue sections as published (Donadoni et al., 2004) using a commercial probe (Cambio). DAPI (4′,6′-diamidino-2-phenylindole) was used to stain the DNA. Combined *Xist* RNA and X chromosome painting was performed sequentially (Chaumeil et al., 2006) using a Cy3-labeled *Xist* probe and a biotin-labeled X paint (Cambio). Images were obtained at room temperature with a fluorescence microscope (Axioplan; Zeiss), a CCD camera (CoolSNAP fx; Photometrics), and MetaMorph image analysis software (Universal Imaging Corp.). Color

levels were adjusted in Photoshop 7.0 (Adobe). All confocal pictures were obtained using a Zeiss LSM 510 Axiovert 200M. Deconvolution microscopy was carried out on a DeltaVision Spectris Restoration Microscopy System (Applied Precision) using a 100× 1.4 NA planachromat lens to collect a series of 0.2 μm z-sections and subsequent deconvolution using the proprietary SoftWorx algorithm (Applied Precision).

Expression Microarray and Bioinformatic Analysis

Total RNA was extracted using Trizol (Invitrogen) and whole genome expression profiles were generated using Affimetrix GeneChip® Mouse Genome 430 2.0 arrays (RZPD, Germany). Data were submitted to the GEO repository using the accession code GSE14585 (http://www.ncbi.nlm.nih.gov/geo/query/acc.cgi?acc=GSE14585). Microarray data were normalized using the Robust Multi-Array Analysis as implemented in Bioconductor (Gentleman et al., 2004; Irizarry et al., 2003). All analyses were performed with log2-transformed data. Hypothesis tests were performed using a modified t statistics with an empirical Bayes approach as implemented in the Bioconductor LIMMA package (Smyth, 2004). The p values were adjusted by the FDR method of Benjamini and Hochberg (1995). Unsupervised hierarchical clustering was performed using the Unweighted Pair Group Method with Arithmetic Mean (UPGMA) and the Pearson correlation coefficient distance measure. A batch effect was removed with a mixed model ANOVA, and all probe sets were ranked by their median absolute deviation. The 300 probe sets with the highest median absolute deviation were selected and z-transformed before clustering.

RNA Interference

NPM-ALK TX/Y R26$^{rtTA/rtTA}$ lymphoma cells were transfected twice with *SATB1* siRNAs (Santa Cruz Biotechnology) or scrambled control siRNAs (Santa Cruz Biotechnology) following the recommendations of the supplier. *Xist* expression was induced by the addition of 1 μg/ml of Doxycycline 48 hr after the first transfection for 5 days. Viable cell number was measured using a CASY® Cell Counter (Schärfe System GmbH). Experiments were performed in triplicate, and error bars plotted represent the standard deviation. For RNA interference in ES cells, 2 × 10^4 cells were plated in a 6-well dish and incubated for 24 hr. Subsequently, cells were transfected using 75 μl/well of 5 μM siRNA (Santa Cruz Biotechnology) and 5 μl/well of Lipofectamlne 2000 (Invitrogen) in OPTI-MEM (GIBCO) without serum. A second round of transfection was performed after 3 days. Cells were then cultured for 48 hr in normal ES medium either with or without Dox and analyzed by northern analysis as described previously (Leeb and Wutz, 2007).

Cloning and Retrovirus Infections

The mouse *SATB1* and human *SATB2* cDNAs (RZPD, Germany) were cloned into the MSCV-CD2 and pBabe-puro vectors. For virus production, Plat-E cells were transfected with these vectors as described (Morita et al., 2000). The supernatant was collected and used for infection of primary or immortalized TX/Y R26$^{rtTA/rtTA}$ mouse embryonic fibroblasts. Infected cells were selected with Puromycin or sorted by FACS after staining with phycoeritrin (PE) anti-human CD2 (eBioscience) using a FACS Aria cell sorter (Becton Dickinson).

ACCESSION NUMBERS

Gene expression profiles have been deposited at GEO with the accession code GEO14585.

SUPPLEMENTAL DATA

Supplemental Data include thirteen figures and two tables and can be found with this article online at http://www.cell.com/developmental-cell/supplemental/S1534-5807(09)00096-3.

ACKNOWLEDGMENTS

We thank Gabi Stengl for FACS analysis, Pavel Pasierbek for help with miroscopy, Johannes Tkadletz for figure preparation, Andreas Bichl and Denise Imre for maintenance of the mouse colony, and Erwin F. Wagner, Denise Barlow, and Joseph Penninger for critically reading the mansucript. We thank Masaru Miyano for thymic cell preparations. This research was supported by a grant from the Vienna Science and Technology Fund (WWTF), by the IMP through Boehringer Ingelheim, and the Austrian Science Fund (FWF). The IMP is funded in part through Boehringer Ingelheim and C.H. is employed by Boehringer Ingelheim.

Received: November 17, 2008
Revised: February 12, 2009
Accepted: March 3, 2009
Published: April 20, 2009

REFERENCES

Alvarez, J.D., Yasui, D.H., Niida, H., Joh, T., Loh, D.Y., and Kohwi-Shigematsu, T. (2000). The MAR-binding protein SATB1 orchestrates temporal and spatial expression of multiple genes during T-cell development. Genes Dev. *14*, 521–535.

Azuma, M., Hirao, A., Takubo, K., Hamaguchi, I., Kitamura, T., and Suda, T. (2005). A quantitative matrigel assay for assessing repopulating capacity of prostate stem cells. Biochem. Biophys. Res. Commun. *338*, 1164–1170.

Benjamini, Y., and Hochberg, Y. (1995). Controlling the false discovery rate: a practical and powerful approach to multiple testing. Journal of the Royal Statistical Society Series, 289–300.

Blewitt, M.E., Gendrel, A.V., Pang, Z., Sparrow, D.B., Whitelaw, N., Craig, J.M., Apedaile, A., Hilton, D.J., Dunwoodie, S.L., Brockdorff, N., et al. (2008). SmcHD1, containing a structural-maintenance-of-chromosomes hinge domain, has a critical role in X inactivation. Nat. Genet. *40*, 663–669.

Britanova, O., Akopov, S., Lukyanov, S., Gruss, P., and Tarabykin, V. (2005). Novel transcription factor Satb2 interacts with matrix attachment region DNA elements in a tissue-specific manner and demonstrates cell-type-dependent expression in the developing mouse CNS. Eur. J. Neurosci. *21*, 658–668.

Britanova, O., Depew, M.J., Schwark, M., Thomas, B.L., Miletich, I., Sharpe, P., and Tarabykin, V. (2006). Satb2 haploinsufficiency phenocopies 2q32-q33 deletions, whereas loss suggests a fundamental role in the coordination of jaw development. Am. J. Hum. Genet. *79*, 668–678.

Brown, C.J., and Willard, H.F. (1994). The human X-inactivation centre is not required for maintenance of X-chromosome inactivation. Nature *368*, 154–156.

Cai, S., Han, H., and Kowhi-Shigematsu, T. (2003). Tissue-specific nuclear architecture and gene function regulated by SATB1. Nat. Genet. *34*, 42–51.

Cai, S., Lee, C.C., and Kohwi-Shigematsu, T. (2006). SATB1 packages densely looped, transcriptionally active chromatin for coordinated expression of cytokine genes. Nat. Genet. *38*, 1278–1288.

Chaumeil, J., Le Baccon, P., Wutz, A., and Heard, E. (2006). A novel role for Xist RNA in the formation of a repressive nuclear compartment into which genes are recruited when silenced. Genes Dev. *20*, 2223–2237.

Chiarle, R., Gong, J.Z., Guasparri, I., Pesci, A., Cai, J., Liu, J., Simmons, W.J., Dhall, G., Howes, J., Piva, R., et al. (2003). NPM-ALK transgenic mice spontaneously develop T-cell lymphomas and plasma cell tumors. Blood *101*, 1919–1927.

Chiarle, R., Voena, C., Ambrogio, C., Piva, R., and Inghirami, G. (2008). The anaplastic lymphoma kinase in the pathogenesis of cancer. Nat. Rev. Cancer *8*, 11–23.

Chow, J.C., Hall, L.L., Baldry, S.E., Thorogood, N.P., Lawrence, J.B., and Brown, C.J. (2007). Inducible XIST-dependent X-chromosome inactivation in human somatic cells is reversible. Proc. Natl. Acad. Sci. USA *104*, 10104–10109.

Clemson, C.M., Hall, L.L., Byron, M., McNeil, J., and Lawrence, J.B. (2006). The X chromosome is organized into a gene-rich outer rim and an internal core containing silenced nongenic sequences. Proc. Natl. Acad. Sci. USA *103*, 7688–7693.

Costanzi, C., and Pehrson, J.R. (1998). Histone macroH2A1 is concentrated in the inactive X chromosome of female mammals. Nature *393*, 599–601.

Csankovszki, G., Panning, B., Bates, B., Pehrson, J.R., and Jaenisch, R. (1999). Conditional deletion of Xist disrupts histone macroH2A localization but not maintenance of X inactivation. Nat. Genet. *22*, 323–324.

Dickinson, L.A., Joh, T., Kowhi, Y., and Kohwi-Shigematsu, T. (1992). A tissue-specific MAR/SAR binding protein with unusual binding site recognition. Cell *70*, 631–645.

Dobreva, G., Dambacher, J., and Grosschedl, R. (2003). SUMO modification of a novel MAR-binding protein, SATB2, modulates immunoglobulin mu gene expression. Genes Dev. *17*, 3048–3061.

Dobreva, G., Chahrour, M., Dautzenberg, M., Chirivella, L., Kanzler, B., Farinas, I., Karsenty, G., and Grosschedl, R. (2006). SATB2 is a multifunctional determinant of craniofacial patterning and osteoblast differentiation. Cell *125*, 971–986.

Donadoni, C., Corti, S., Locatelli, F., Papadimitriou, D., Guglieri, M., Strazzer, S., Bossolasco, P., Salani, S., and Comi, G.P. (2004). Improvement of combined FISH and immunofluorescence to trace the fate of somatic stem cells after transplantation. J. Histochem. Cytochem. *52*, 1333–1339.

Galande, S., Purbey, P.K., Notani, D., and Kumar, P.P. (2007). The third dimension of gene regulation: organization of dynamic chromatin loopscape by SATB1. Curr. Opin. Genet. Dev. *17*, 408–414.

Gentleman, R.C., Carey, V.J., Bates, D.M., Bolstad, B., Dettling, M., Dudoit, S., Ellis, B., Gautier, L., Ge, Y., Gentry, J., et al. (2004). Bioconductor: open software development for computational biology and bioinformatics. Genome Biol. *5*, R80.

Hall, L.L., Byron, M., Sakai, K., Carrel, L., Willard, H.F., and Lawrence, J.B. (2002). An ectopic human XIST gene can induce chromosome inactivation in postdifferentiation human HT-1080 cells. Proc. Natl. Acad. Sci. USA *99*, 8677–8682.

Han, H.J., Russo, J., Kohwi, Y., and Kohwi-Shigematsu, T. (2008). SATB1 reprogrammes gene expression to promote breast tumour growth and metastasis. Nature *452*, 187–193.

Hoflinger, S., Kesavan, K., Fuxa, M., Hutter, C., Heavey, B., Radtke, F., and Busslinger, M. (2004). Analysis of Notch1 function by in vitro T cell differentiation of Pax5 mutant lymphoid progenitors. J. Immunol. *173*, 3935–3944.

Huynh, K.D., and Lee, J.T. (2003). Inheritance of a pre-inactivated paternal X chromosome in early mouse embryos. Nature *426*, 857–862.

Irizarry, R.A., Bolstad, B.M., Collin, F., Cope, L.M., Hobbs, B., and Speed, T.P. (2003). Summaries of Affymetrix GeneChip probe level data. Nucleic Acids Res. *31*, e15.

Keohane, A.M., O'Neill, L.P., Belyaev, N.D., Lavender, J.S., and Turner, B.M. (1996). X-Inactivation and histone H4 acetylation in embryonic stem cells. Dev. Biol. *180*, 618–630.

Krivtsov, A.V., Twomey, D., Feng, Z., Stubbs, M.C., Wang, Y., Faber, J., Levine, J.E., Wang, J., Hahn, W.C., Gilliland, D.G., et al. (2006). Transformation from committed progenitor to leukaemia stem cell initiated by MLL-AF9. Nature *442*, 818–822.

Leeb, M., and Wutz, A. (2007). Ring1B is crucial for the regulation of developmental control genes and PRC1 proteins but not X inactivation in embryonic cells. J. Cell Biol. *178*, 219–229.

Marahrens, Y., Panning, B., Dausman, J., Strauss, W., and Jaenisch, R. (1997). *Xist*-deficient mice are defective in dosage compensation but not spermatogenesis. Genes Dev. *11*, 156–166.

Mermoud, J.E., Costanzi, C., Pehrson, J.R., and Brockdorff, N. (1999). Histone macroH2A1.2 relocates to the inactive X chromosome after initiation and propagation of X-inactivation. J. Cell Biol. *147*, 1399–1408.

Morita, S., Kojima, T., and Kitamura, T. (2000). Plat-E: an efficient and stable system for transient packaging of retroviruses. Gene Ther. *7*, 1063–1066.

Morris, S.W., Kirstein, M.N., Valentine, M.B., Dittmer, K.G., Shapiro, D.N., Saltman, D.L., and Look, A.T. (1994). Fusion of a kinase gene, ALK, to a nucleolar protein gene, NPM, in non-Hodgkin's lymphoma. Science *263*, 1281–1284.

Penny, G.D., Kay, G.F., Sheardown, S.A., Rastan, S., and Brockdorff, N. (1996). Requirement for *Xist* in X chromosome inactivation. Nature *379*, 131–137.

Plath, K., Fang, J., Mlynarczyk-Evans, S.K., Cao, R., Worringer, K.A., Wang, H., de la Cruz, C.C., Otte, A.P., Panning, B., and Zhang, Y. (2003). Role of histone H3 lysine 27 methylation in X inactivation. Science *300*, 131–135.

Rasmussen, T.P., Mastrangelo, M.A., Eden, A., Pehrson, J.R., and Jaenisch, R. (2000). Dynamic relocalization of histone MacroH2A1 from centrosomes to inactive X chromosomes during X inactivation. J. Cell Biol. *150*, 1189–1198.

Sado, T., Fenner, M.H., Tan, S.S., Tam, P., Shioda, T., and Li, E. (2000). X inactivation in the mouse embryo deficient for Dnmt1: distinct effect of hypomethylation on imprinted and random X inactivation. Dev. Biol. *225*, 294–303.

Sado, T., Okano, M., Li, E., and Sasaki, H. (2004). De novo DNA methylation is dispensable for the initiation and propagation of X chromosome inactivation. Development *131*, 975–982.

Savarese, F., Flahndorfer, K., Jaenisch, R., Busslinger, M., and Wutz, A. (2006). Hematopoietic precursor cells transiently reestablish permissiveness for X inactivation. Mol. Cell. Biol. *26*, 7167–7177.

Schoeftner, S., Sengupta, A.K., Kubicek, S., Mechtler, K., Spahn, L., Koseki, H., Jenuwein, T., and Wutz, A. (2006). Recruitment of PRC1 function at the initiation of X inactivation independent of PRC2 and silencing. EMBO J. *25*, 3110–3122.

Smyth, G.K. (2004). Linear models and empirical bayes methods for assessing differential expression in microarray experiments. Stat. Appl. Genet. Mol. Biol. *3*, Article3.

Wen, J., Huang, S., Rogers, H., Dickinson, L.A., Kohwi-Shigematsu, T., and Noguchi, C.T. (2005). SATB1 family protein expressed during early erythroid differentiation modifies globin gene expression. Blood *105*, 3330–3339.

Wutz, A., and Jaenisch, R. (2000). A shift from reversible to irreversible X inactivation is triggered during ES cell differentiation. Mol. Cell *5*, 695–705.

Wutz, A., Rasmussen, T.P., and Jaenisch, R. (2002). Chromosomal silencing and localization are mediated by different domains of Xist RNA. Nat. Genet. *30*, 167–174.